Electrical and Structural Properties of $CuBa_2LaCa_2Cu_4O_{11+\delta}$ Superconducting System

Mohammed Abdul-nebi Thejeel[1], Maher A. Hasan[2], Haider MJ. Haider[3], Kareem Ali Jasim[4*]

Abstract

In this work, the superconducting $CuBa_2LaCa_2Cu_4O_{11+\delta}$ compound was prepared by citrate precursor method and the electrical and structural properties were studied. The electrical resistivity has been measured using four probe test to find the critical temperature $T_{c(offset)}$ and $T_{c(onset)}$. It was found that $T_{c\ (offset)}$ at zero resistivity has 101 K and $T_{c\ (onset)}$ has 116 K. The X-ray diffraction (XRD) analysis exhibited that a prepared compound has a tetragonal structure. The crystal size and microscopic strain due to lattice deformation of $CuBa_2LaCa_2Cu_4O_{11+\delta}$ were estimated by four methods, namely Scherer(S), Halder-Wagner(H-W), size-strain plot (SSP) and Williamson-Hall, (W-H) methods. Results of crystal sizes obtained by these methods were compared with each other. In all these methods, the values of β_{hkl} (full-width half-maximum (FWHM) for diffraction peaks) and miler indices (hkl) are determined from the results obtained from Fullprof, Mach, Origin and VESTA software. The lattice parameters a, b and c, lattice shape, d and degree of crystallization were calculated. It was found that the crystal size which are calculating by S, W-H, SSP and H-W were (174.8472, 171.1776, 173.1009 and 175.4386) A^0 respectively while the lattice strain values were (none, 0.0025, 0.004 and 0.003464), respectively.

Key Words: Citrate Precursor Method, X-ray Diffraction, Full-width Half-maximum, Halder Wagner, Scherer, Size-Strain Plot and Williamson-Hall Method.

DOI Number: 10.14704/nq.2022.20.1.NQ22012 **NeuroQuantology 2022; 20(1):90-96**

Introduction

Superconductors and their technologies have significant benefits in our lives. The superconducting materials have significant improvements in efficiency and performance in many industrial, medical and technological devices such as medical devices, computers and communications. In addition that, the ability of superconducting materials to generate, transmits and store electrical energy; therefore they are used as environmentally friendly transportation tools (L. Shahadan, M., Suan, M., Johan, 2013; Jasim K.A., 2014).

Superconductivity is a phenomenon based on quantum theory that some materials display when cooled to low temperatures. The superconductors at critical temperature allow a constant electrical current to flow without loss due to zero resistance.

Corresponding author: Kareem Ali Jasim

Address: [1]Department of Physics, College of Education for Pure Sciences Ibn Al-Haitham, University of Baghdad, Iraq; [2]Ministry of Education, Tikrit Directorate of Education, Salah Aldin, Iraq; [3]Physics Department, Faculty of Education for Girls, Kufa University, Iraq; [4*]Department of Physics, College of Education for Pure Sciences Ibn Al-Haitham, University of Baghdad, Iraq;

E-mail: [1]mohammed.a.t@ihcoedu.uobaghdad.edu.iq; [2]bmahereabd@yahoo.com; [3]alhaidery83@yahoo.com;

[4*]Kareem.a.j@ihcoedu.uobaghdad.edu.iq

Relevant conflicts of interest/financial disclosures: The authors declare that the research was conducted in the absence of any commercial or financial relationships that could be construed as a potential conflict of interest.

Received: 08 November 2021 **Accepted:** 13 December 2021

The large and powerful superconducting magnets are used in science, medical, research, technology development (Kareem. A. Jasim, Tariq J. Alwan, 2011; Shahadan, M., Suan, M., Rafie, M., Chua Siang, 2012). In addition, ultra-low AC losses in superconductors may lead to significant energy savings in power applications (A. Mendonc¸, T.M. Tavares, P.B. Correia, J.G. Lopes, A.M.L., Darie, C., Araujo, 2011; Jasim, 2012). Superconducting devices are considered optimum choice to use them many different life fields because they have higher currents, fields and magnetic forces, higher energy density, smaller volume (Li, J., Wu, Y., Pan, Y., Guo, 2007; J. Chandradass, 2009).

Researchers in this field are racing to find high-temperature superconducting materials for their multiple applications. One of these materials is beryllium-calcium copper oxide with the chemical formula $CuBa_2LaCa_2Cu_4O_{11-\delta}$ that is one of the homogeneous compounds (C.J. Liu, C.Q. Jin, 1996). The system $CuBa_2LaCa_2Cu_4O_{11-\delta}$ is considered within superconducting phases having high transition temperature at around 90-92 K, and which match superconductor of Hg-based coppers (H.A. Mook, P. Dai, 2000). The cuprate superconductor $CuBa_2Ca_3Cu_4O_{11-\delta}$ (Cu-1234) with T_c= 117 K has recently been synthesized using high-pressure (C.Q. Jin, S. Adachi, X.J. Wu, H. Yamauchi, 1994; Abbas K. Saadon, Kareem A. Jasim, 2020; Kassim Mahdi Wadi, Kareem A. Jasim, Auday H. Shaban, Mustafa K. Kamil, 2020; Mustafa K. Kamil and Kareem A. Jasim, 2020; Mustafa K. Kamil1, Maher A. Hasan, 2021). Polycrystalline samples were fabricated by the researchers from $CuBa_2Ca_3Cu_4O_{11-\delta}$ by reaction annealing at 950°C and under pressure of 5 GPa for one hour using starting materials of BaO, CaO and CuO with stoichiometric composition. The electrical resistance was measured using the four standard probes , where they found the zero critical temperature $T_{c(offset)}$ equal to 115.9 K and the transformation degree from normal to superconducting state $T_{c(onset)}$ is 117 K, while the X-ray diffraction analysis showed that the crystal structure is quaternary and that the lattice constants a = 3.859Å and c = 18.00Å (C.Q. Jin, S. Adachi, X.J. Wu, H. Yamauchi, 1994).

The present work aims to prepare the $CuBa_2LaCa_2Cu_4O_{11+\delta}$ superconducting phase using the acetate-tartrate solution method and to study the crystal sizes and stresses that occur during the preparation of the compound by different calculation methods.

Preparation

$CuBa_2LaCa_2Cu_4O_{11}$ sample has been prepared by an acetate-tartrate solution method. We used the raw materials of La_2O_3, Cu $(CH_3COO)_4 H_2O$, $Ca(CH_3COO)_2 H_2O$ and Ba $(CH_3COO)_2$ according to stoichiometric amounts. Firstly, La_2O_3 was dissolved in acetic acid solution at 0.2 M in a beaker covered using magnetic stirrer for time 10 h and temperature 50-60°C, where solution is obtained. The second step, appropriate amounts of Ba $(CH_3COO)_2$, Ca $(CH_3COO)_2 H_2O$, and $Cu(CH_3COO)_4 H_2O$, then they dissolved in appropriate amount of distilled water by stirring to 6 h at the same temperature. For preventing crystallization of metal acetate during gel formation, acid was added to the reaction mixture through control the pH to 5.6. Using slow evaporation of an open beaker 10 h at 70°C the concentrated solution was obtained. When approximately 85% of the water has been evaporated with constant stirring, a transparent blue gel is formed. After further drying in an oven at 90°C, a fine blue powder is obtained. The result powders were placed in an alumina crucible for calcination for 10 h at 860°C in flowing oxygen, then carefully re-collected in agate slurry, and then heated again for 6 hours at 800°C, after another grinding step. The powder was pressed using hydraulic press into a disc shape of 15 mm in diameter and 3 mm thick. Finally, the superconducting compound was obtained by annealing the sample for 4 h at 500°C in oxygen.

A prepared sample structure was obtained using X-ray diffraction (XRD). Both the crystal size and the strain were calculated by the angles and widths of the intensity of the XRD peaks. XRD results were refined by Fullprof, Mach, Origin and VESTA software, to calculate lattice parameters a, shape of lattice, d space, (FWHM) and Degree of crystallinity. The crystallite size was estimated by SSP, W–H and H–W methods and the results for obtained by these methods were compared with Scherer results.

Results and Discussion

1. Resistivity

The electrical resistivity measurements versus temperature, represented in Figure 1, confirmed the existence of superconducting phases. The sample prepared by the acetate-tartrate solution method had critical temperatures within the range (T_c = 101-116 K). Where it is observed that electrical resistance decreases with decreasing temperatures and this indicates that the sample has a metallic

behavior. The sample shows a near-linear temperature dependence on the resistance, where zero resistance can be clearly observed, it shows at $T_{c(onset)}$= 116 K, and the beginning of the transition from the normal state to the superconducting was found at 101 K, although the critical temperature values are very similar.

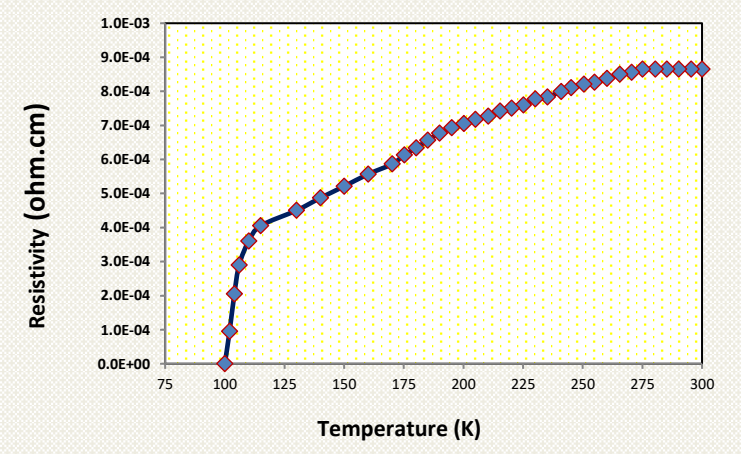

Figure 1. The Resistivity dependence on Temperature for $CuBa_2LaCa_2Cu_4O_{11+\delta}$ sample with $T_{coffset}$ 101K

2. Structure

The diffraction spectrum is a function of the change in the intensity of the diffraction of X-rays in terms of the angle θ through a specific crystal structure. Through the study and analysis of this spectrum, several properties related to the crystal can be obtained, the most important of which are the structure of the crystal lattice: lies in knowing the basic cell lattice constants of the crystal and knowing γ, β, α and c, b, a Miller's coefficients for diffraction levels (hkl). This information can be obtained by using the 2θ values of the hkl diffraction angles causing these peaks (Warren, B.E.; Averbach, 1952; Jacob, R.; Isac, 2015; Nath, D.; Singh, F.; Das, 2020).

The position of atoms in the basic cell by studying the electron density, especially when crystals with polyatomic compounds. This density is translated through the shape of the crest and the intensity of the diffracted rays. By integrating the results (determining the lattice + determining the position of the atoms (the base)), we can know the crystal structure. In addition to knowing the crystal structure, other properties of crystals can be determined through X-ray diffraction, such as the size of the crystals (Mustafa K. Kamil and Kareem A. Jasim, 2020).

Figure (2) shows the XRD patterns taken for the sample and according to the X-ray diffraction data the prepared sample consists of an almost pure polycrystalline Cu-1224 phase (Marked with H) and small amounts of Cu-1213, Cu-1202 phase (Marked with L) were present in sample, with very small amount of impurity phases of $CaCu_2O_3$ and Ca_2CuO_3 at the end of the chart. The results show a compound with a perovskite structure with a tetragonal structure. The results of the crystal lattice parameters that were obtained from applying Barack's law and using the Origin software are: a = 3.8425 A^0, c = 3.8427 A^0 and c = 17.9741 A^0. XRD results were refined by Mach! Origin and VESTA software, to calculate lattice parameters, crystal size, d space, (FWHM) and Degree of crystallinity.

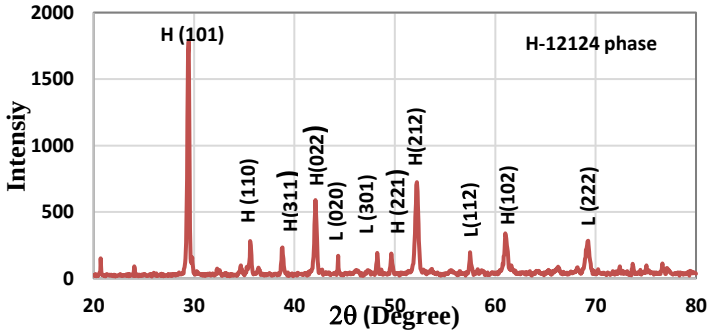

Figure 2. X-ray diffraction of $CuBa_2LaCa_2Cu_4O_{11+\delta}$ sample

2.1. Calculation of Crystal Size by Use Shearer's Equation

Science Shearer has developed an equation in 1918 to calculate the dimensions of nanoparticles when knowing the Bragg angle and the width of its highest diffraction spectrum line, in which the crystal size (D) is inversely proportional to the full width measurement of half-maximal peaks β, the higher the spectral line width, the smaller the crystal size and vice versa (Riyadh Kamil Chillab, Sarab Saadi Jahil, Kassim Mahdi Wadi, Kareem A. Jasim, 2021). It is given by the following relationship (Kassim Mahdi Wadi, Kareem A. Jasim, Auday H. Shaban, Mustafa K. Kamil, 2020):

$$D = \frac{K\lambda}{\beta.cos\theta} \qquad (1)$$

Where wavelength is λ (nm), half-maximal peaks (β) in radians. The form factor (k) is 0.9. The aim of the Scherrer modified equation used in this work is to reduce sources of errors when the least squares technique can be applied. According to the Scherrer equation, we can plots cosθ versus 1/ β_{hkl}. It is possible to obtain from the best slope of the line that passes through the narrowest points in the figure 3, which represents the relationship Kλ/D, from which one value (average) of D is obtained by all available peaks is 174.8472 A^0, and that the value of R^2 is equal to 0.7602 as shown in figure 3.

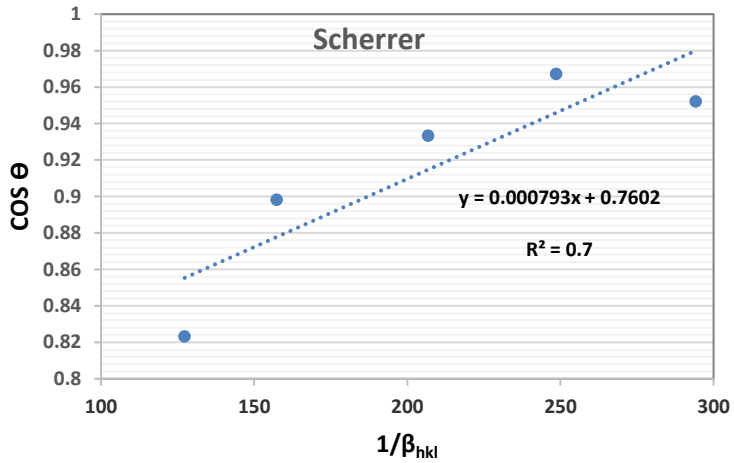

Figure 3. Cosθ as a function of $1/ß_{hkl}$ of $CuBa_2LaCa_2Cu_4O_{11+\delta}$ presented by Scherer's equation

2.2. Crystallite Size and Strain Using W-H Method

This method is another equation for calculating the crystal size and the strain which can be created during the preparation process. From this relationship and with help of the X-ray diffraction plot we can us the following equation (Balzar, D.; Ledbetter, 1993).

$$\beta_{hkl}cos\theta = \frac{k\lambda}{D} + 4\,\varepsilon\, sin\,(\theta) + \beta o \qquad (2)$$

Where D, ε, β_o represents crystallite size, strain and instrumental broadening respectively. A linear equation can be drawn between β_{hkl} cosθ versus 4sinθ for $CuBa_2LaCa_2Cu_4O_{11+\delta}$ sample as shown in Fig. 4, where the Y axis represents β_{hkl} cosθ and X axis represents 4 sinθ. This graph shows that the slope of the straight line represents an intrinsic strain value, which is found to be 0.0025. While its intersection with the Y-axis gives the average crystal size, which was found to be 171.1776 A^0 and that the value of R^2 is equal to 0.8697, the Table indicates their values. By comparing the two equations 1 and 2, we note that the average grain size using the W-H equation is greater than the grain size average using the Debye-Scherer equation, where the W-H equation took into account the strain effect of the grains, where the reason for the width of the peaks is attributed to the size of the grains and the internal strain at the same time, which is small when powders are used (Balzar, D.; Ledbetter, 1993).

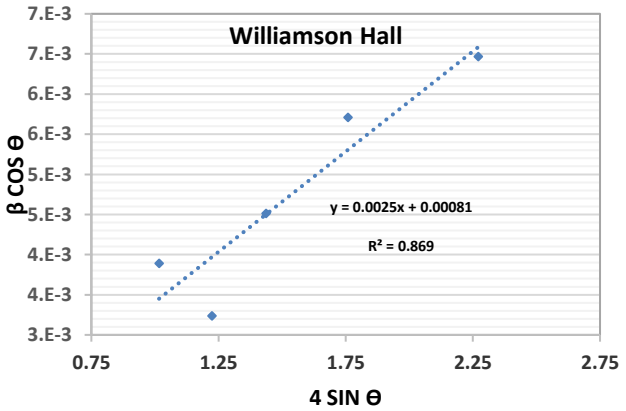

Figure 4. β_{hkl} cosθ versus 4sinθ for $CuBa_2LaCa_2Cu_4O_{11+\delta}$ calculated from W-H method

2.3. Size Strain Plot (SSP) Method

The XRD data depending on the high reflections angles in this method be less considering. Since higher angles and higher modulation, it has a better result of isotropic broadening, where the XRD data is of lower quality and the peaks overlap. In this assumption, using the strain profile by the Gaussian function and the crystal size by the Lorentzian function, the profile is explained (Mazhidi, M.; Khani, 2008; Kassim Mahdi Wadi, Kareem A. Jasim, Auday H. Shaban, Mustafa K. Kamil, 2020). Moreover, the overall scalability of this method was expressed by Eq. (3).

$$\beta_{hkl} = \beta_L + \beta_G \quad (3)$$

Where, β_L and βG are the peak broadening via functions of Lorentz and Gaussian consequently. Equation (4) is the submitted formula of the SSP method (Mazhidi, M.; Khani, 2008).

$$(d_{hkl}B_{hkl}\,cos\theta)^2 = \frac{k\lambda}{D}(d^2{}_{hkl}B_{hkl}\,cos\theta) + \left(\frac{\varepsilon}{2}\right)^2 \quad (4)$$

Figure 5 illustrates the relationship between to $(d\beta_{hkl}\cos\theta)^2$ on the y-axis and to $d^2\beta_{hkl}\cos\theta$ on the x-axis in application of equation 4, where the slope of the straight line represents the first fixed term $(\frac{k\lambda}{D})$ of the equation, while we get the second term $\left(\frac{\varepsilon}{2}\right)^2$ from its point of intersection with the y-axis, and that the value of R^2 is equal 0.6823. After extracting the slope and its intersection value with the y-axis and compensating each of the wavelengths and k, the crystal size was obtained, which is equal to 173.1009 A^0, while the strain is equal to 0.004.

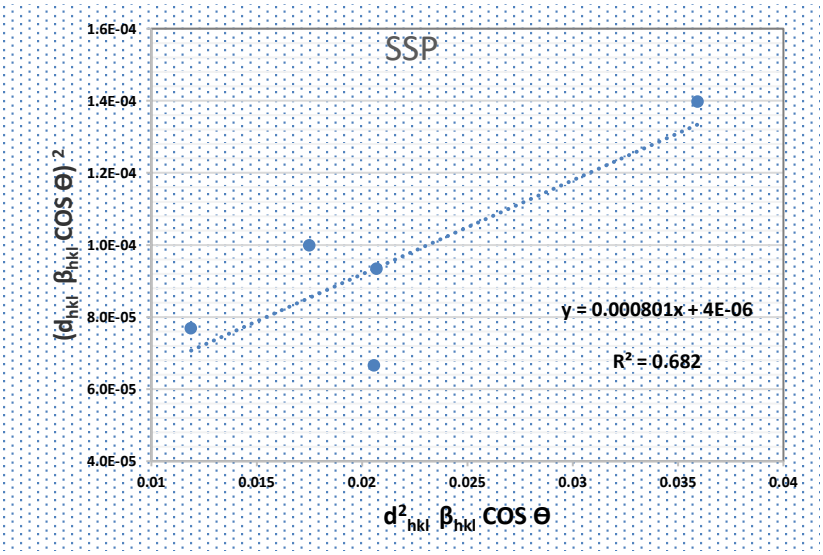

Figure 5. $(d_{hkl}\beta_{hkl}\cos\theta)^2$ versus $d^2{}_{hkl}\beta_{hkl}\cos\theta$ of $CuBa_2LaCa_2Cu_4O_{11+\delta}$ calculated from SSP

2.4. Halder-Wagner (H-W) Method

Halder and Wagner proposed another equation to determine D and strain (Mote, V.D.; Purushotham, Y.; Dole, 2012). It is containing the integral width (β) of a reciprocal lattice and the lattice plane spacing(d) of the reciprocal cell. In this method, the relationship between strain and crystallite size is given by (M., 2011; Prabhu, Y.T.; Rao, K.V.; Kumar, V.S.S.; Kumari, 2014)

$$\left(\frac{\beta^*_{hkl}}{d^*_{hkl}}\right)^2 = \left(\frac{k}{D}\right)\left(\frac{\beta^*_{hkl}}{d^{*2}_{hkl}}\right) + (2\varepsilon)^2 \quad (5)$$

Where $\beta^*{}_{hkl} = \left(\frac{\beta_{hkl}.cos\phi}{\lambda}\right)$ and $d^*{}_{hkl} = \left(2d_{hkl}\frac{sin\phi}{\lambda}\right)$. Equation (5) has the form of a straight line, y = ax + b. In the Halder–Wagner (H-W) diagram, y is plotted for $y = (\beta^*{}_{hkl})/(d^*{}_{hkl})^2$ and $x = \beta^*{}_{hkl}/d^{*2}_{hkl}$. Then, the slope and y-intercept of the resulting straight line provide K/D and $2\varepsilon^2$, respectively. Although estimates and assumptions have been made regarding the derivation of the equation 5, the H-W scheme has the significant advantage of the lower and middle angles reflectance data more important compared with those at angles of higher diffraction, which are often less reliable. From figure 6, the crystal size was obtained, which equal to 175.4386 A^0, while the strain is equal to 0.003464.

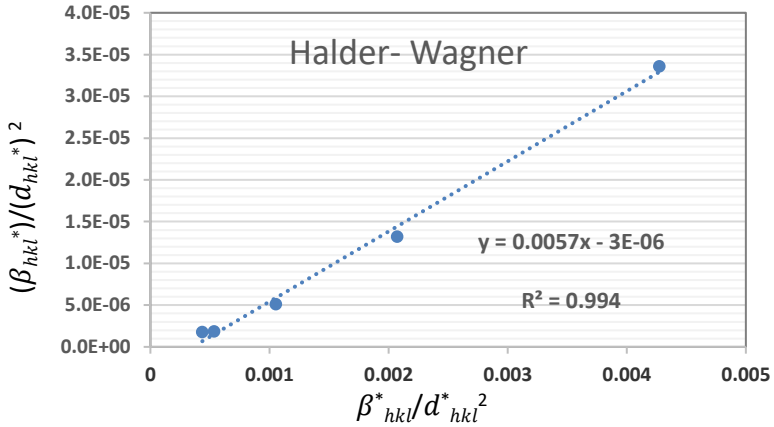

Figure 6. $(\beta^*_{hkl})/(d^*_{hkl})^2$ versus $\beta^*_{hkl}/d^{*2}_{hkl}$ of $CuBa_2LaCa_2Cu_4O_{11+\delta}$ calculated from H-W method.

The table (1) shows Crystallite size and lattice strain of $CuBa_2LaCa_2Cu_4O_{11+\delta}$ sample according to X-ray diffraction chart and using different four Methods. Figure 7 represents the results of the crystallite sizes obtained from the four methods (Mohammed Abdul-Nebi, Rihab Nassr Fadhil, Shatha. H. Mahdie, Kareem A. Jasim, 2021; Raghad Subhi Abbas Al-Khafaji, 2021). It is noted from this figure that the lowest value of the crystalline size was calculated by Williamson-Hall method, in it was the highest value calculated by the Halder-Wagner method. This result is considered the best because the values of R^2 in it are close to one.

Table 1. Crystallite size and lattice strain of $CuBa_2LaCa_2Cu_4O_{11+\delta}$ sample by different Methods.

parameters	Scherrer	Williamson Hall	SSP	Halder Wagner
Crystallite size	174.8472 A⁰	171.1776A⁰	173.1009A⁰	175.4386A⁰
strain	none	0.0025	0.004	0.003464

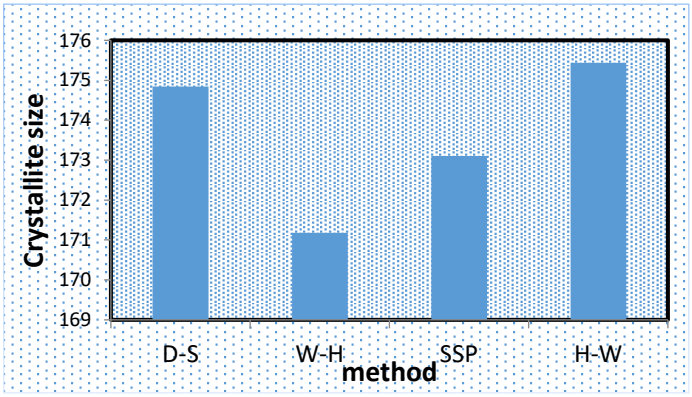

Figure 7. Crystallite size of different Method for $CuBa_2LaCa_2Cu_4O_{11+\delta}$ sample

Crystallity

The degree of crystallization can be measured using crystallography using an X-ray diffraction chart based on the equation mentioned in references (Mohammed Abdul-Nebi, Rihab Nassr Fadhil, Shatha. H. Mahdie, Kareem A. Jasim, 2021; Raghad Subhi Abbas Al-Khafaji, 2021) where X-ray diffraction is used to assess and know the degree of crystallization of many crystalline materials. Crystallization is generally calculated as a percentage of the crystalline volume by applying Equation (6) and using VESTA Software, it was found that the degree of crystallization was 60.33 %.

$$Crystallinity = \frac{Aera\ of\ Crystalline\ peaks}{Aera\ of\ all\ peaks\ (Crystalline+Amorphus)}\ x\ 100 \qquad (6)$$

Conclusion

In this work, the electrical and structural properties of the compound $CuBa_2LaCa_2Cu_4O_{11+\delta}$ superconductor prepared by an acetate-tartrate solution technique were studied. The electrical

resistivity was examined as a function of temperature and it was found that the critical temperature $T_{c\ (onset)}$ (starting) at 116K and the critical temperature at zero resistance $T_{c\ (off\ set)}$ is 101 K, and the change in transition width (ΔT = 15 K). Examination of the structure and characterization of the X-ray powder diffraction pattern. Using Fullprof software confirms that a tetragonal structure is valid. Moreover, the results of crystal size and strain (using Mach and Origin) estimated by SSP, Scherrer, W-H, and H-W methods show that H-W method is more accurate and better than other methods because the value of R^2 is close to 1. The degree of crystallization was calculated by using VESTA software confirms that equal to 60. 33 %.

References

Mendonça TM, Tavares PB, Correia JG, Lopes AML, Darie C, Araújo JP. The urea combustion method in the preparation of precursors for high-TC single phase HgBa2Ca2Cu3O8+ δ superconductors. *Physica C: Superconductivity* 2011; 471(23-24): 1643-1646.

Saadon AK, Jasim KA, Shaban AH. Superconducting Compound Hg0. 8Sb0. 2Ba2Ca2Cu3O8+ δ Compared with Hg0. 8Sb0. 2Ba2Ca1Cu2O6+ δ to Evaluate Transition Temperature. *NeuroQuantology* 2020; 18(11): 14-18.

Balzar D, Ledbetter H. Voigt-function modeling in Fourier analysis of size-and strain-broadened X-ray diffraction peaks. *Journal of Applied Crystallography* 1993; 26(1): 97-103.

Liu CJ, Jin CQ, Yamauchi H. Thermoelectric power of high-pressure synthesized $CuBa_2Ca_3Cu_4O_{11}-\delta$. *Physical Review B* 1996; 53(9): 5170- 5173.

Jin CQ, Adachi S, Wu XJ, Yamauchi H, Tanaka S. 117 K superconductivity in the Ba-Ca-Cu-O system. *Physica C: Superconductivity* 1994; 223(3-4): 238-242.

Mook HA, Dai P, Dogan F, Hunt RD. One-dimensional nature of the magnetic fluctuations in $YBa_2Cu_3O6.6$. *Nature* 2000; 404(6779): 729-731.

Chandradass J, Kim KH. Effect of acidity on the citrate-nitrate combustion synthesis of alumina-zirconia composite powder. *Metals and Materials International* 2009; 15(6): 1039-1043.

Jacob R, Isac J. X-ray diffraction line profile analysis of $Ba0.6Sr0.4FexTi(1-x)\ O3-\delta$,(x= 0.4). *International Journal of Chemical Studies* 2015; 2: 12-21.

Jasim KA. Superconducting Properties of Hg 0.8 Cu 0.15 Sb 0.05 $Ba_2Ca_2Cu3O_8+\delta$ Ceramic with Controlling Sintering Conditions. *Journal of superconductivity and novel magnetism* 2012; 25(6): 1713-1717.

Jasim KA, Thejeel MA, Al-Khafaji RS. The Effect of Doping by Sr on the Structural, Mechanical and Electrical Characterization of La1Ba1-xSrx $Ca_2Cu_4O_8$. 5+δ. *Ibn AL-Haitham Journal For Pure and Applied Science* 2017; 27(1), 170-175.

Jasim KA, Alwan TJ, Al-Lamy HK, Mansour HL. Improvements of superconducting properties of Hg 0.6 Pb 0.25 Sb 0.15Ba^2 $Ca^2Cu^3O^8$+δ ceramic by controlling the sintering time. *Journal of superconductivity and novel magnetism* 2011; 24(6): 1963-1966.

Wadi KM, Jasim KA, Shaban AH, Kamil MK, Nsaif FK. The Effects of Sustainable Manufacturing Pressure on the Structural Properties of the $Pb_2Ba_2Ca_2Cu_3O_9+\sigma$ Compound. *Journal of Green Engineering* 2020; 10: 6052-6062.

Suan MSM, Johan MR. Synthesis of Al_2O_3 nanoparticles highly distributed in $YBa_2Cu_3O_7$ superconductor by citrate–nitrate auto-combustion reaction. *Physica C: Superconductivity* 2013; 492: 49-54.

Li J, Wu Y, Pan Y, Guo J. Influence of citrate-to-nitrate ratio on the thermal behavior and chemical environment of alumina gel. *Ceramics international* 2007; 33(5): 735-738.

Theivasanthi T, Alagar M. Nano sized copper particles by electrolytic synthesis and characterizations. *International Journal of Physical Sciences* 2011; 6(15): 3662-3671.

Mazhdi M, Hossein KP. Structural characterization of ZnO and ZnO: Mn nanoparticles prepared by reverse micelle method. *International Journal of Nano Dimension* 2012; 2(4): 233-240.

Thejeel MAN, Fadhil RN, Mahdie SH, Jasim KA, Shaban AH. Effect of Partial Substitution of Sr by Ba on the Structural Properties of $Tl0._8Ni0._2Sr_2$-xBrxCa_2Cu_3O9-δ System. *In Key Engineering Materials* 2021; 900: 172-179.

Mote VD, Purushotham Y, Dole BN. Williamson-Hall analysis in estimation of lattice strain in nanometer-sized ZnO particles. *Journal of theoretical and applied physics* 2012; 6(1): 1-8.

Kamil MK, Jasim KA. Calculating of crystalline size, strain and Degree of crystallinity of the compound ($HgBa_2Ca_2Cu_3O_8$+ σ) by different method. *In IOP Conference Series: Materials Science and Engineering* 2020; 928(7).

Kamil MK, Hasan MA, Jasim KA, Shaban AH. Synthesis of $HgSr_2$-xYx$Ca_2Cu_3O_8$+δ Superconducting Compound. *In Key Engineering Materials* 2021; 886: 42-47.

Nath D, Singh F, Das R. X-ray diffraction analysis by Williamson-Hall, Halder-Wagner and size-strain plot methods of CdSe nanoparticles-a comparative study. *Materials Chemistry and Physics* 2020; 239.

Prabhu YT, Rao KV, Kumar VSS, Kumari BS. X-ray analysis by Williamson-Hall and size-strain plot methods of ZnO nanoparticles with fuel variation. *World Journal of Nano Science and Engineering* 2014; 4(1): 21-28.

Al-Khafaji RSA, Jasim KA. Dependence the microstructure specifications of earth metal lanthanum La substituted $Bi_2Ba_2CaCu_2$–$XLaXO_8$ on cation vacancies. order, *AIMS Materials Science* 2021; 8(4): 550-559.

Chillab RK, Jahil SS, Wadi KM, Jasim KA, Shaban AH. Fabrication of $Ge_3$0Te 70-xSbx Glasses Alloys and Studying the Effect of Partial Substitution on DC Electrical Energy Parameters. *In Key Engineering Materials* 2021; 900: 163-171.

Suan MSM, Johan MR, Siang TC. Synthesis of Y3Ba5Cu8O18 superconductor powder by auto-combustion reaction: effects of citrate–nitrate ratio. Physica C: Superconductivity, 2012; 480: 75-78.

Warren BE, Averbach BL. The separation of cold-work distortion and particle size broadening in X-ray patterns. *Journal of applied physics* 1952; 23(4), 497-497.

Khalaph KA, Jafar AM. Lead-free two-dimensional perovskite solar cells cs_3 fe_2 cl_9 using mgo nanoparticulate films as hole transport material. *NeuroQuantology* 2020; 18(2): 127-132.